OBSERVATIONS AND ANALYSIS OF LUNAR RADIO EMISSION AT 3.09 mm WAVELENGTH*

BOBBY L. ULICH,** JOHN R. COGDELL, and JOHN H. DAVIS
Millimeter Wave Observatory, The University of Texas, Austin, Tex., U.S.A.

and

TED A. CALVERT
Space Sciences Laboratory, NASA Marshall Space Flight Center, Huntsville, Ala., U.S.A.

(Received 23 July, 1973)

Abstract. Observations of lunar radio emission were made at 3.09 mm wavelength (97.1 GHz) from April 18 to May 20, 1971. Absolute brightness temperatures were measured for five distinct areas – Copernicus, Sea of Serenity, Sea of Tranquility (Apollo 11 landing site), Ocean of Storms (Apollo 12 landing site), and a highland region near the mean center – and lunation curves were determined. Theoretical brightness temperatures throughout a lunation were calculated for Copernicus, Sea of Serenity, and the Highlands region using a thermophysical model employing variable properties of the lunar soil. The results showed that the predicted lunation curves are quite sensitive to the value of the electric loss tangent. The model for the loss tangent which best fits the observed data is significantly different from that describing particulate basalt. Calculations were also made for comparison with earlier observations at the same frequency of the total lunar eclipse on February 10, 1971. Variations in the observed eclipse and lunation curves between regions are sufficiently great to prevent matching all the observations with a single model.

1. Introduction

Many authors have made significant contributions to both experimental and theoretical aspects of lunar microwave emission. Reviews of this area have been presented by Weaver (1965), Hagfors (1971), and Muhleman (1972). Efforts to construct a theoretical model to satisfactorily predict both eclipse and lunation temperatures have been hindered by a lack of knowledge of the physical temperature distribution beneath the lunar surface, the physical properties of the lunar soil, and perhaps the effects of surface slopes.

Observations of lunar radio emission have previously been reported by Gary *et al.* (1965), Low and Davidson (1965), Gibson (1958), Troitskii *et al.* (1967), and others. These studies have contributed greatly to the understanding of the physical properties of the Moon. However, such practices as averaging data taken over many lunations to obtain a single lunation curve, using single scans of the lunar disk to derive a lunation curve, presenting the data in harmonic form, and omitting absolute temperature calibration of the data have complicated attempts to construct a satisfactory model. The experimental data analyzed in this paper were obtained in such a way as to facilitate comparison with a calculated model. The data were taken during a

* The antenna system is supported by NASA Grant NGL 44-012-006.
** Presently at the National Radio Astronomy Observatory, Tucson, Ariz., U.S.A.

The Moon **10** (1974) 163–174.

single lunation and no averaging was performed. Specific regions of the Moon were studied with enough angular resolution to distinguish between different types of terrain. The data were absolutely calibrated and yield a new measurement of the lunation average brightness temperature of the center of the Moon, which is important for calibration of other sources (Linsky, 1973, and Ulich *et al.*, 1973).

2. Observations

The 4.88 m diam parabolic antenna at the Millimeter Wave Observatory (elevation 2070 m) on Mt. Locke, Texas was used to make the observations. The antenna half power beamwidth at 97.1 GHz is 2.52′. The radio telescope is equatorially mounted, and digital position encoders have a resolution of 3.6″. Absolute pointing accuracy is better than 15″ maximum error.

Efficiency losses due to spillover, spar blockage, scattering, and radiometer blockage have been calculated to be 7.6, 3.5, 1.3 and 0.6% respectively, at 3.09 mm wavelength, giving a beam efficiency of $87.5 \pm 2.2\%$. This efficiency is the antenna coupling factor to a uniformly bright disk of the same angular diameter as the Moon. The brightness temperature of the Sun at 3.09 mm, determined using this coupling efficiency, is 6815 ± 310 K (Ulich *et al.*, 1973). The total absolute calibration error for extended sources is estimated to be less than 4%. The receiver was a standard superheterodyne Dicke radiometer located at the prime focus; its sensitivity was 3.8 K RMS for an integration time of one second.

Five regions of the lunar surface were chosen for observation. Three of them – Copernicus, Sea of Serenity, and the Highlands – represent distinct types of lunar terrain and have been observed during a total eclipse at the same frequency (Ulich, 1972). Copernicus and its surrounding rays are a relatively recent crater system. The Sea of Serenity is a relatively smooth mare region, and the Highlands area represents the mountainous terrain. The areas around the landing sites for Apollo 11 and Apollo 12 were chosen since comparisons with *in situ* and returned sample measurements are possible. Antenna positions for the five regions were predetermined with corrections for librations, refraction (Davis and Cogdell, 1970), and mount eccentricities (Davis and Cogdell, 1969). Observations were made on 30 days between April 18, 1971 and May 20, 1971, during lunation number 598.

Antenna temperatures were measured using an OFF-ON-OFF (SKY-MOON-SKY) technique. Each baseline observation lasted 80 seconds, and each lunar observation lasted 160 s. Integrated digital data were recorded every 10 s. The antenna temperature scale was periodically determined by injecting a signal from a thermally calibrated neon noise tube. Each cycle of observing the five sites and a calibration required about 45 min to complete, allowing approximately eight complete cycles during each observing period. Atmospheric extinction data were taken using drift scans of the Sun for periods when the Moon was in the daytime sky. Near full Moon observations of the Moon were made at low elevation angles, and these data were used to calculate the extinction.

The radiometer digital output, the time of each data set, the antenna position, and auxiliary information were recorded on punched paper tape. The data were converted to punched cards and analyzed on a digital computer. Voltage deflections for each OFF-ON-OFF observation were converted to antenna temperatures by comparison with the noise tube calibration signal. The noise tube equivalent antenna temperature of 80 ± 2 K was previously determined by comparison with a well matched termination thermally cycled between boiling water and ice slush. Linear interpolation was used between calibration points. Antenna positions were used to calculate the air mass corresponding to each observation, and corrections for atmospheric extinction were made in the usual manner (Shimabukuro, 1966). Corrected antenna temperatures were then converted to brightness temperatures using the calculated beam coupling efficiency.

3. Theoretical Calculations

Early analyses by Piddington and Minnett (1949) and by Troitskii (1954) produced an expression of the following type to describe the thermal emission from the Moon at radio wavelengths

$$T_B(\lambda, t) = [1 - R(\theta_0)] \int_0^\infty T(x, t)\, K(\lambda, x) \sec\theta(x, \theta_0) \times \exp\left[- \int_0^x K(\lambda, \xi) \sec\theta(\xi, \theta_0)\, d\xi \right] dx, \quad (1)$$

where

T_B = Brightness temperature (K)
λ = Wavelength (m)
t = Time (sec)
R = Fresnel reflection coefficient at the surface
θ_0 = Angle between the normal to the surface and the line of sight to the observer
T = Physical temperature
x = Depth beneath surface (m)
K = Power absorption coefficient (m^{-1})
θ = Angle between the normal to the surface and the refracted ray in the absorbing medium

The calculations presented here have been made using Equation (1) and incorporating available information on the variable thermophysical properties of the lunar soil. The electrical properties have been shown to be functions of wavelength, temperature, and density (Katsube and Collett, 1971, and Chung *et al.*, 1971). However, these effects are not well defined for the lunar soil at millimeter wavelengths; consequently, studies of terrestrial basalt powder (Wechsler, 1971) at 3.24 cm and 1.18 cm were assumed to account for the effect of a variable density. The temperature dependence

is uncertain and was ignored in this analysis. The calculations assume the density of the uppermost layer to be represented by the model of Jones (1968), in which the density increases with depth beneath the lunar surface. The studies of basalt powder by Wechsler (1971) revealed that for values of the dessity ϱ from 0.6 to 1.6 gm/cm^3, the relative dielectric constant ε and loss tangent $\tan\delta$ are represented by

$$\varepsilon(x) = 0.74 + 1.6\varrho(x), \tag{2}$$

$$\tan\delta(x) = 0.0029 + 0.0038\varrho(x). \tag{3}$$

Both parameters are depth dependent since they vary with the density which is depth dependent. The power absorption coefficient K may be expressed in the usual form

$$K(\lambda, x) = \frac{2\pi}{\lambda}\sqrt{\varepsilon(x)}\tan\delta(x). \tag{4}$$

The reflection coefficient R at the surface ($x=0$) is determined from the Fresnel relationships for parallel and perpendicular polarization of the radiation as

$$R(\theta_0) = R_{\parallel}(0, \theta_0)\cos^2\gamma + R_{\perp}(0, \theta_0)\sin^2\gamma, \tag{5}$$

where

$$R_{\parallel}(x, \theta_0) = \left[\frac{\varepsilon(x)\cos\theta_0 - \sqrt{\varepsilon(x) - \sin^2\theta_0}}{\varepsilon(x)\cos\theta_0 + \sqrt{\varepsilon(x) - \sin^2\theta_0}}\right]^2, \tag{6}$$

$$R_{\perp}(x, \theta_0) = \left[\frac{\cos\theta_0 - \sqrt{\varepsilon(x) - \sin^2\theta_0}}{\cos\theta_0 + \sqrt{\varepsilon(x) - \sin^2\theta_0}}\right]^2; \tag{7}$$

and γ is the polarization angle of the emitted radiation, measured clockwise from the north in the plane of projection. The angle θ is determined by Snell's law of refraction

$$\theta(x, \theta_0) = \sin^{-1}\left[\frac{\sin\theta_0}{\sqrt{\varepsilon(x)}}\right]. \tag{8}$$

Numerical values of $T(x, t)$ and $\varrho(x)$ were supplied by Jones *et al.* (1973) from their model which best matches the observed infrared emission. A computer program using the relationships presented here and the physical temperature profiles presented by Jones *et al.* (1973) was used to evaluate Equation (1) for comparison with the observations.

4. Results

Good observing conditions allowed daily observations of all five regions during a complete lunation with the exception of two days. Brightness temperatures were calculated and a lunation curve was established for each site. Daily brightness temperatures are given in the Appendix. Plots of brightness temperature versus fraction of a lunation period (FOP), reckoned from full Moon, are given in Figures 1-5. The brightness temperatures of all sites were between 318K maximum and 153K minimum. Maximum temperature readings occurred in general at approximately 0.075

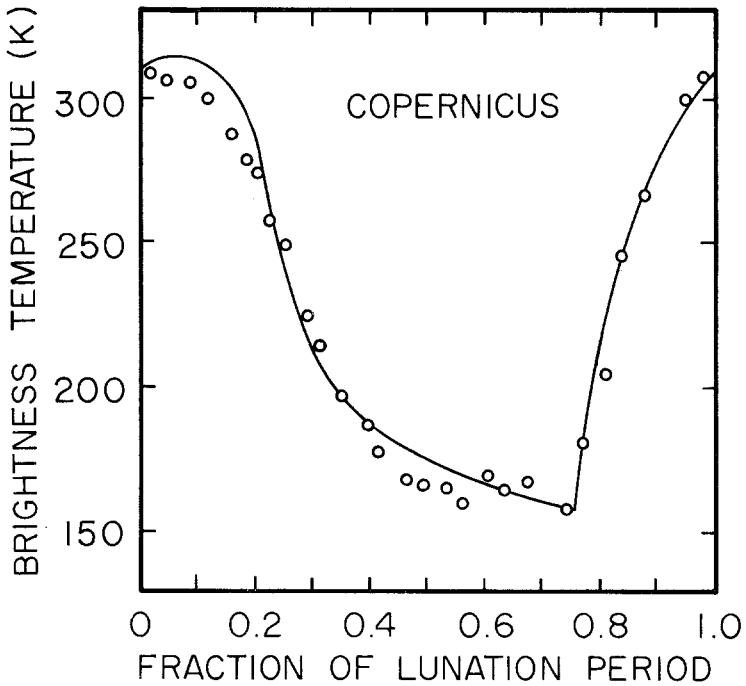

Fig. 1. 3.09 mm Lunation data for Copernicus with theoretical curve.

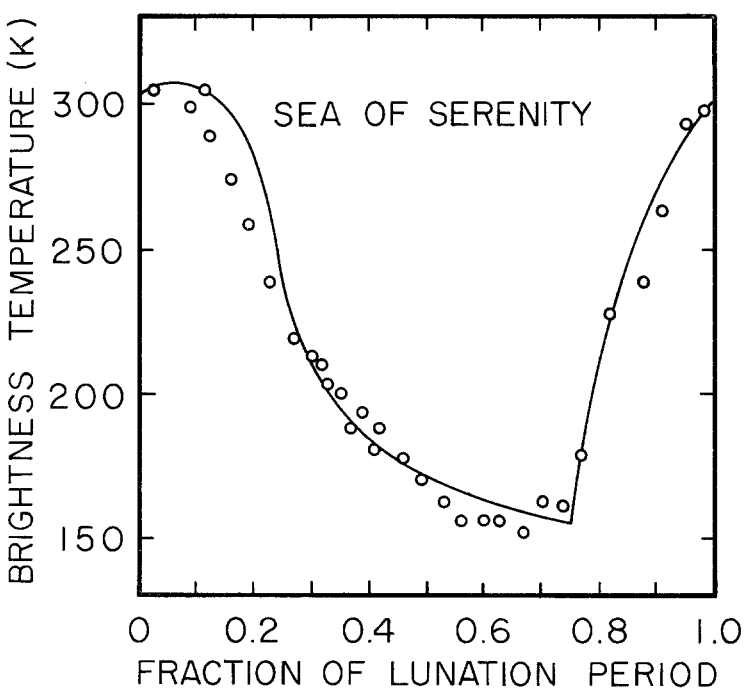

Fig. 2. 3.09 mm Lunation data for Sea of Serenity with theoretical curve.

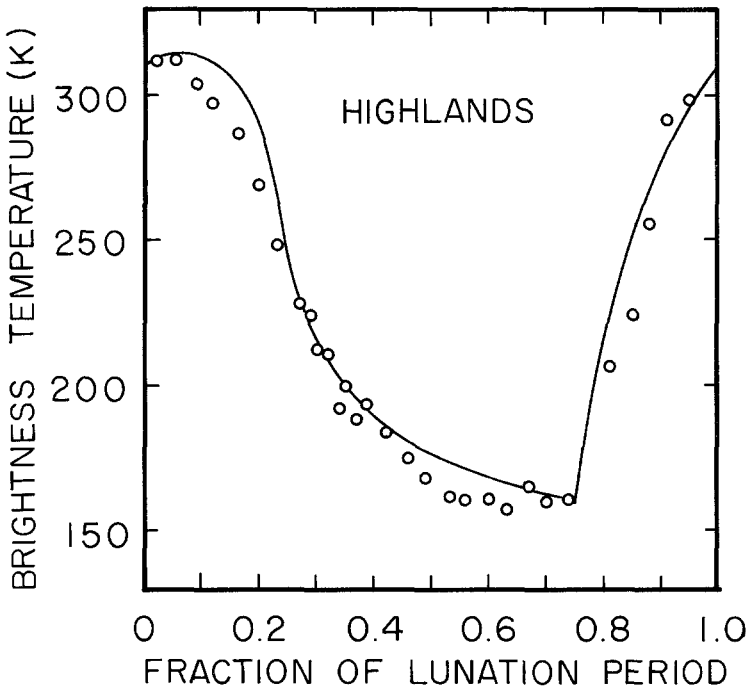

Fig. 3. 3.09 mm Lunation data for Highlands with theoretical curve.

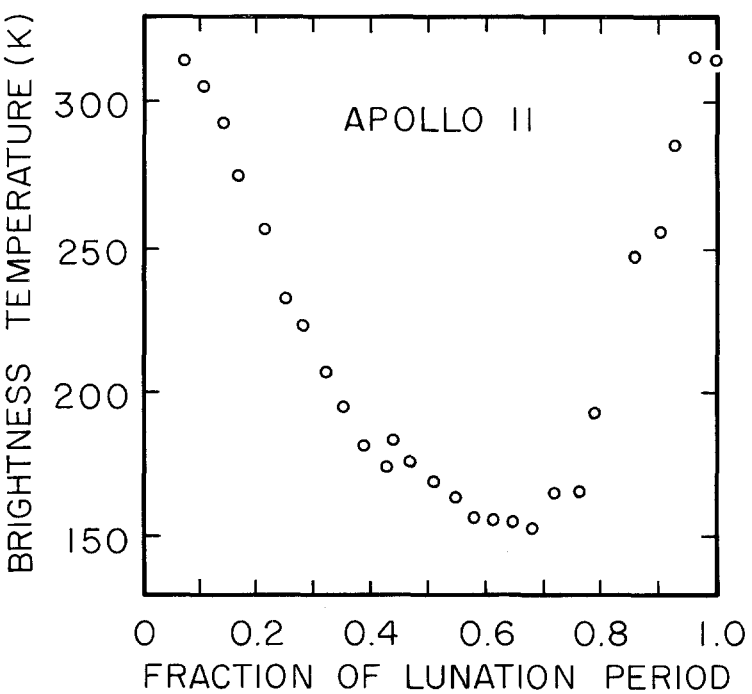

Fig. 4. 3.09 mm Lunation data for Apollo 11.

FOP, which corresponds to a phase lag of 27°. The lunation average brightness temperature of the Highlands region, which is quite near the mean center of the Moon, was found to be 223±8K, and at new Moon the Highlands brightness temperature was 165±6K. Cooling rates for Copernicus and Apollo 12 were less than the other sites in the 0.1 to 0.2 FOP range. During this part of the lunation, the temperatures of Copernicus and Apollo 12 declined more slowly, producing a more rounded curve than the other sites.

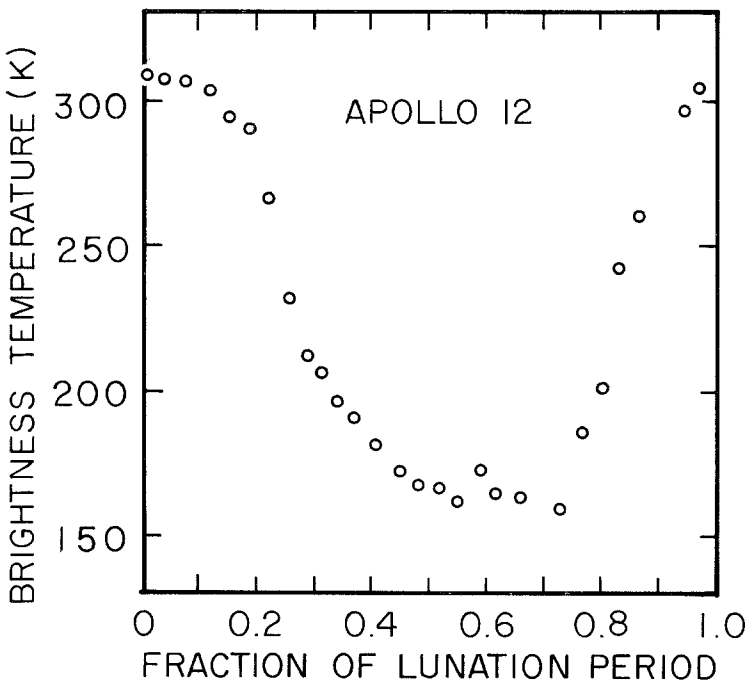

Fig. 5. 3.09 mm Lunation data for Apollo 12.

In addition to the observed data, Figures 1–3 show theoretical curves of brightness temperature during the lunation calculated using Equation (1). These theoretical lunation curves were selected to best fit the observations using values of the relative dielectric constant and the loss tangent within the range of values commonly accepted as representing the lunar soil. The assumed variation of density with depth is given in Figure 6.

In making the initial calculations, two points concerning the loss tangent became apparent. The first was that the values of the loss tangent determined from studies of basalt powders (Wechsler, 1971) produce calculated brightness temperatures which are lower than the observational data. The second was the manner in which slight changes in the magnitude of the loss tangent produce significant changes in the calculated temperatures. As a result the loss tangent was allowed to be a free parameter

in the calculations and was varied by trial and error to determine theoretical curves comparable to the observed brightness temperatures. The magnitude of the loss tangent was varied by simply changing the coefficients of Equation (3). For Copernicus, Sea of Serenity, and the Highlands areas, the most suitable lunation curves are calculated with a loss tangent of the form

$$\tan \delta(x) = 0.013 + 0.004\varrho(x). \tag{9}$$

For Copernicus this produced a maximum brightness temperature of 314 K, a minimum temperature of 159 K, and a 25° phase lag. When the constant term of Equation (9) is decreased, the maximum temperature decreases and the minimum temperature

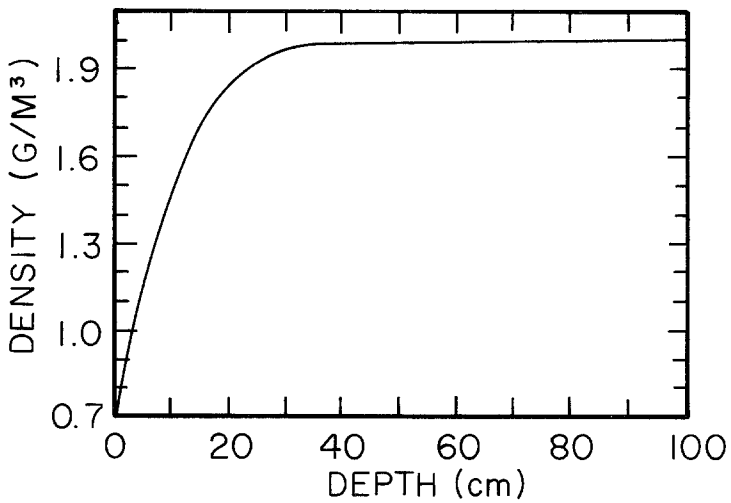

Fig. 6. Variation of lunar soil density with depth beneath the surface.

and phase lag increase. This demonstrates that the loss tangent is an important factor in the theory of millimeter lunar emission and underscores the need to more accurately determine its functional dependence. In the density range of Figure 6 the loss tangent calculated from Equation (9) varies from 0.016 to 0.021. This range is acceptable in view of the measurements of Apollo fine grained material by Katsube and Collett (1971). Their measurements were made between 10^3 and 10^7 Hz, and although the analysis here is directed toward much higher frequencies, it is interesting to note how well the values determined here compare with the values measured for the Apollo fines.

Values of the relative dielectric constant in the range commonly accepted for fine grained lunar material do not greatly influence the calculated lunation curves. Brightness temperatures for all sites were calculated using the relative dielectric constant given by Equation (2).

In addition to calculations of lunation temperatures, calculations were also made for comparison with previous eclipse observations by Ulich (1972) which have been

revised upward based upon a more accurate thermal calibration of the receiver. These calculations were made for Copernicus, Sea of Serenity, and the Highlands sites observed by Ulich and used the same physical temperature profile, density, loss tangent, and relative dielectric constant as the lunation calculations. Only the variation in solar insolation due to the difference in time from February to April, 1971 was allowed. Comparisons of the theoretical eclipse curves with the observations are shown in Figures 7 and 8. The Highlands data compare reasonably well with the calculated eclipse curve. Pre-eclipse brightness temperatures averaged near 312K and fell to a minimum of 286K. Immediately following the eclipse the calculated temperature is 303K, whereas the observations indicate a brightness temperature near 310K. The

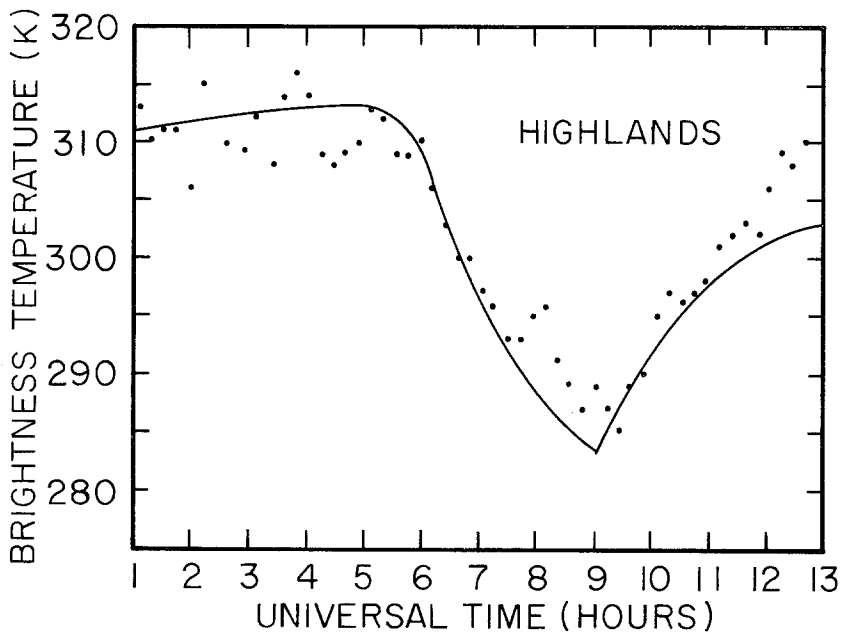

Fig. 7. Eclipse data for Highlands with theoretical curve (Ulich, 1972).

calculated brightness temperatures for Copernicus prior to the eclipse are 10K higher than the observed values but agree better during and after the eclipse. The observations and theoretical eclipse curve for the Sea of Serenity are similar to those of Copernicus. In general, the calculated lunation curves fit the observations better than the calculated eclipse curves.

5. Conclusions

Observations of the Moon's millimeter brightness temperature during a lunation can be duplicated by theoretical calculations with considerable success using the physical temperature profile from a model which is consistent with observations of infrared emission during both the lunar day and a lunar eclipse. Our analysis showed the luna-

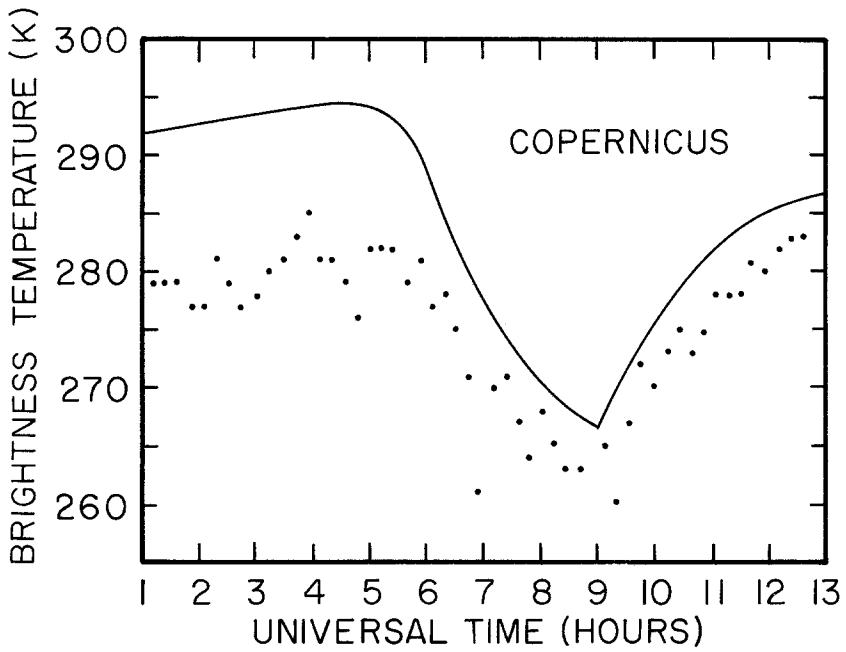

Fig. 8. Eclipse data for Copernicus with theoretical curve (Ulich, 1972).

tion curves to be quite sensitive to the magnitude and functional dependence of the loss tangent. The model for the loss tangent best fitting the lunation data is significantly different from that describing basalt powder. The sensitivity of the calculations to changes in the loss tangent points out the importance of further studies of the dielectric properties of the lunar material, particularly at millimeter wavelengths.

The model best fitting the lunation data resulted in a reasonable fit to the eclipse data. However, the lunation and eclipse curves for the separate regions of the Moon are sufficiently different to prevent matching all the regions with a single model. A unique determination of the electrical properties of each region cannot be made until a more sophisticated model is developed utilizing a dependence of the thermophysical properties on temperature, wavelength, density, and particle size.

TABLE I

Selenographic coordinates of observed regions

Site	Name	Selenographic longitude (°)	Selenographic latitude (°)
1	Copernicus	−19.98	9.62
2	Sea of Serenity	18.17	26.10
3	Highlands	5.80	−8.63
4	Apollo 11	24.43	0.69
5	Apollo 12	−23.41	−3.04

TABLE II

3.09 mm brightness temperatures for lunation number 598 in 1971

Universal time			Site 1		Site 2		Site 3		Site 4		Site 5	
Month	Day	Hour	FOP	T_B(K)	FOP	T_B(K)	FOP	T_B(K)	FOP	T_B(K)	FOP	T_B(K)
4	18	14	0.214	275	0.319	211	0.285	225	0.336	210	0.204	220
4	19	14	0.248	250	0.353	201	0.319	212	0.370	199	0.238	216
4	20	15	0.283	226	0.388	195	0.354	200	0.405	188	0.273	209
4	21	16	0.318	214	0.424	190	0.390	195	0.440	185	0.309	206
4	22	16	0.352	197	0.457	177	0.424	185	0.474	177	0.343	196
4	23	16	0.386	187	0.491	171	0.457	174	0.508	170	0.376	191
4	24	18	0.422	179	0.528	163	0.494	169	0.545	166	0.413	182
4	25	18	0.456	170	0.562	157	0.528	162	0.579	158	0.447	172
4	26	19	0.492	166	0.597	156	0.563	160	0.614	157	0.482	168
4	27	20	0.527	166	0.632	156	0.599	160	0.649	158	0.518	167
4	28	21	0.562	160	0.668	153	0.634	158	0.684	155	0.553	163
4	29	21	0.596	170	0.702	165	0.668	166	0.718	167	0.587	174
4	30	23	0.633	165	0.738	163	0.704	161	0.755	168	0.623	165
5	1	23	0.667	168	0.772	180	0.738	162	0.789	194	0.657	164
5	4	2	0.739	159	0.844	228	0.810	208	0.861	249	0.729	159
5	5	3	0.774	181	0.879	239	0.845	226	0.896	256	0.765	186
5	6	3	0.808	206	0.913	264	0.879	257	0.930	287	0.799	202
5	7	3	0.842	247	0.947	295	0.913	292	0.964	318	0.832	243
5	8	4	0.877	267	0.982	298	0.948	299	0.999	317	0.868	260
5	10	5	0.946	300	0.051	306	0.018	312	0.068	316	0.937	297
5	11	6	0.981	307	0.087	298	0.053	313	0.103	307	0.972	306
5	12	8	0.018	309	0.123	289	0.090	305	0.140	294	0.009	310
5	13	8	0.052	306	0.157	275	0.123	297	0.174	277	0.043	308
5	14	9	0.087	306	0.193	259	0.159	287	0.209	258	0.080	308
5	15	11	0.124	300	0.229	239	0.195	270	0.246	234	0.115	304
5	16	12	0.159	289	0.265	220	0.231	248	0.281	215	0.150	295
5	17	13	0.194	280	0.300	213	0.266	230	0.316	209	0.185	289
5	18	13	0.228	259	0.334	204	0.300	213	0.350	197	0.219	266
5	19	14	0.263	221	0.369	188	0.335	193	0.386	182	0.255	232
5	20	16	0.300	202	0.406	181	0.372	189	0.422	176	0.291	211

Appendix

The lunar radio observations reported here are averages of the emission over a substantial area of the lunar surface. The region viewed by the main beam at the half power level is a circle about 280 km in diam. The theoretical calculations described, however, are strictly valid only for a single point on the lunar surface. Table I gives the selenographic coordinates of the observed regions which were used to calculate the antenna positions, the fraction of a lunation period (FOP), and the theoretical lunation curves for each site. Table II gives the observed brightness temperatures versus both Universal Time and FOP.

References

Chung, D., Westphal, W., and Simmons, G.: 1971, 'Dielectric Behavior of Lunar Samples: Electro-Magnetic Probing of the Lunar Interior', in A. A. Levinson (ed.), *Proceedings of the Second Lunar Science Conference*, pp. 2381–2390.

Davis, J. H. and Cogdell, J. R.: 1969, *Pointing of the 16 Foot Antenna*, University of Texas at Austin, Elec. Eng. Res. Lab. Technical Memo, NGL-006-6.

Davis, J. H. and Cogdell, J. R.: 1970, *IEEE Trans. Antennas Propagation* **AP-18**, 490.

Gary, B., Stacey, J., and Drake, F.: 1965, *Astrophys. J. Suppl. Ser.* **12**, 239.

Gibson, J.: 1958, *Proc. IRE* **46**, 280.

Hagfors, T.: 1971, 'Microwave Studies of Thermal Emission from the Moon', in Z. Kopal (ed.), *Advances in Astronomy and Astrophysics*, Academic Press, New York, pp. 1–28.

Jones, B.: 1968, *J. Geophys. Res.* **73**, 7631.

Jones, B. P., Calvert, T., and Watkins, J.: 1973, 'Temperatures and Thermophysical Properties of the Lunar Outermost Layer', to be published.

Katsube, T. and Collett, L.: 1971, 'Electrical Properties of Apollo 11 and Apollo 12 Lunar Samples', in A. A. Levinson (ed.), *Proceedings of the Second Lunar Science Conference*, pp. 2381–2390.

Linsky, J. L.: 1973, *Astrophys. J. Suppl. 216* **26**, 1.

Low, F. and Davidson, A.: 1965, *Astrophys. J.* **142**, 1278.

Muhleman, D.: 1972, 'Microwave Emission from the Moon', in J. Lucas, (ed.), *Thermal Characteristics of the Moon*, MIT Press, Cambridge, pp. 51–81.

Piddington, J. and Minnett, H.: 1949, *Australian J. Sci. Res.* **A2**, 63.

Shimabukuro, F. I.: 1966, *IEEE Trans. Antenna Propagation* **AP-14**, 228.

Troitskii, V. S.: 1954, *Astron Zh.* **31**, 511.

Troitskii, V. S., Krotikov, V. D., and Tseitlin, N. M.: 1967, *Sov. Astron. AJ* **11**, 327.

Ulich, B. L.: 1972, *Icarus* **16**, 304.

Ulich, B. L., Cogdell, J. R., and Davis, J. H.: 1973, *Icarus* **19**, 59–82.

Weaver, H.: 1965, 'The Interpretation of Thermal Emission from the Moon', in J. Aarons, (ed.), *Solar System Radio Astronomy*, Academic Press, New York, pp. 295-354.

Wechsler, A.: 1971, 'Dielectric Properties of Basalt Powders', Final report to NASA, G. C. Marshall Space Flight Center, Contract No. NAS8-25119, A. D. Little, Inc.